nature immunology

Activation of bone marrow–resident memory T cells by circulating, antigen-bearing dendritic cells

Lois L Cavanagh[1,5,6], Roberto Bonasio[1,5], Irina B Mazo[1], Cornelia Halin[1], Guiying Cheng[1], Adrianus W M van der Velden[2], Annaiah Cariappa[3], Catherine Chase[3], Paul Russell[3], Michael N Starnbach[2], Pandelakis A Koni[4], Shiv Pillai[3], Wolfgang Weninger[1,6] & Ulrich H von Andrian[1]

Dendritic cells (DCs) carry antigen from peripheral tissues via lymphatics to lymph nodes. We report here that differentiated DCs can also travel from the periphery into the blood. Circulating DCs migrated to the spleen, liver and lung but not lymph nodes. They also homed to the bone marrow, where they were retained better than in most other tissues. Homing of DCs to the bone marrow depended on constitutively expressed vascular cell adhesion molecule 1 and endothelial selectins in bone marrow microvessels. Two-photon intravital microscopy in bone marrow cavities showed that DCs formed stable antigen-dependent contacts with bone marrow–resident central memory T cells. Moreover, using this previously unknown migratory pathway, antigen-pulsed DCs were able to trigger central memory T cell–mediated recall responses in the bone marrow.

Dendritic cells (DCs) are key participants in innate and adaptive immune responses[1]. The prevalent model of DC migration is an unidirectional pathway whereby precursor DCs arise from progenitors in the bone marrow, enter the blood and traffic into secondary lymphoid organs and peripheral tissues, such as skin or gut[2], where they contribute to the front line of defense against pathogens. When DCs encounter inflammatory stimuli, they undergo a switch in chemokine receptor expression, enabling their egress into lymphatic vessels and transport to draining lymph nodes[3]. Maturing DCs also become fully immunostimulatory by upregulating major histocompatibility complex (MHC) and costimulatory molecules to prime naive T cells.

Normal peripheral blood contains some immature DCs, which capture blood-borne bacteria and transport them to the spleen[4]. However, whether these DCs originate directly in the bone marrow or reenter the blood after migrating within other tissues is unclear. There is ample experimental evidence that draining lymph nodes are the terminal targets for most DCs that leave peripheral tissues. However, a few observations suggest that tissue-resident DCs can somehow return to the blood and carry antigen to organs other than lymph nodes. For example, DCs carry fluorescent beads, dyes or antigen to the spleen after either intracutaneous injection or instillation into the lung[5–7]. However, whether and to what extent blood-borne DCs carry antigen to other tissues is unclear. This question has clinical relevance, as in cancer vaccine trials, autologous DCs modified *ex vivo* have been infused into patients[8]. The migration of DCs to nonlymphoid organs might be advantageous for 'boosting' memory responses to previously encountered pathogens, as antigen-experienced T cells disseminate to many nonlymphoid tissues[9]. Different organs contain T cells with distinct functional properties. The bone marrow is particularly notable in this; $CD8^+$ memory cells in bone marrow undergo more vigorous homeostatic proliferation and respond faster to antigen stimulation than those in other tissues[10,11]. The bone marrow actively accumulates $CD8^+$ central memory T cells (T_{CM} cells), which are more frequent among T cells in the bone marrow than elsewhere[12]. In cancer patients, memory T cells in the bone marrow have greater antitumor reactivity than do peripheral blood memory cells[13]. However, it is unclear whether and how recall antigen from tumors or pathogens gains access to the bone marrow.

Here we report that small numbers of DCs traffic constitutively from peripheral tissues to blood. Moreover, circulating DCs have considerable bone marrow tropism. Using intravital microscopy in mouse skull bone marrow, we show that homing of DCs to the bone marrow depended on microvascular P-selectin and E-selectin as well as vascular cell adhesion molecule 1 (VCAM-1). Once in the bone marrow, DCs induced rapid proliferation of antigen-specific T_{CM} cells. Using two-photon intravital microscopy to visualize T cell receptor (TCR)–transgenic T_{CM} cells and DCs that had homed to bone marrow cavities, we found that both cell types rarely interacted in the absence of antigen, whereas antigen-presenting DCs rapidly formed stable conjugates with T_{CM} cells. These data suggest a pathway for DC migration that allows DCs to collect antigen in peripheral sites and then traffic to the bone marrow to elicit recall responses by resident T_{CM} cells.

[1]The CBR Institute for Biomedical Research and Department of Pathology and [2]Department of Microbiology and Molecular Genetics, Harvard Medical School, Boston, Massachusetts 02115, USA. [3]Massachusetts General Hospital Cancer Center, Charlestown, Massachusetts 02129, USA. [4]Institute of Molecular Medicine and Genetics, Medical College of Georgia, Augusta, Georgia 30912, USA. [5]These authors contributed equally to this work. [6]Present address: The Wistar Institute, Philadelphia, Pennsylvania 19104, USA. Correspondence should be addressed to U.H.v.A. (uva@cbr.med.harvard.edu).

Received 13 June; accepted 8 August; published online 11 September 2005; doi:10.1038/ni1249

RESULTS

In vivo migration pathways of DCs

Our first objective was to elucidate the trafficking routes of differentiated DCs after adoptive transfer into the circulation of normal mice. To obtain a sufficiently large number of DCs for these experiments, we expanded DC populations *in vivo* by implanting donor mice with tumors secreting the ligand for the cytokine receptor Flt3 (refs. 14,15). At about 2 weeks after tumor implantation, donor splenocytes yielded large numbers of $CD11c^+$ cells representing every conventional DC subset[15]. Donor DCs uniformly displayed an immature phenotype (MHC class II^{int}, $CD80^{lo}$, $CD86^{lo}$ and $CCR7^{lo}$). Maturation was induced by 24–48 h of culture in lipopolysaccharide (LPS), as demonstrated by upregulation of MHC and costimulatory molecules (**Table 1**).

After injecting tail veins, we analyzed the distribution of donor DCs in recipient blood and tissues by flow cytometry (**Fig. 1a**). At 2 h after injection of both immature and mature DCs (**Fig. 1b**), we recovered the largest numbers from the liver, followed by the lung and the spleen. At 24 h after injection (**Fig. 1b**), immature DCs were retained to a greater extent than mature DCs in the liver, while the number of immature and mature DCs in the lung had dropped by 90% and 95%, respectively. Unexpectedly, there was also substantial accumulation of preferentially immature DCs in the recipients' bone marrow. At 2 h after injection, the number of immature and mature DCs in the bone

Table 1 Adhesion and activation molecule expression in immature and mature DCs

	$CD11c^+CD8\alpha^-$		$CD11c^+CD8\alpha^+$	
Adhesion molecule	Immature	Mature	Immature	Mature
CD11a (α_L)[a]	1,154 ± 214 (99.3)	562 ± 3 (89.7)	2,056 ± 387 (99.9)	1,387 ± 334 (98.5)
CD11b (α_M)	1,002 ± 209 (78.7)	453 ± 56 (62.3)	245 ± 50 (42.3)	942 ± 302 (37.3)
CD49d (α_4)[b]	284 ± 63 (94.6)	306 ± 16 (78.0)	293 ± 57 (97.9)	348 ± 28 (70.7)
CD49e (α_5)	139 ± 39 (57.8)	175 ± 9 (56.3)	176 ± 47 (81.9)	492 ± 55 (41.9)
CD18 (β_2)	1,618 ± 403 (100)	634 ± 18 (97.1)	2,453 ± 489 (100)	1,216 ± 263 (97.6)
CD61 (β_3)	96 ± 19 (57.1)	60 ± 6 (25.1)	45 ± 9 (15.7)	70 ± 4 (8.1)
β_7	162 ± 45 (80.4)	107 ± 9 (40.5)	187 ± 5 (95.8)	155 ± 7 (34.8)
$\alpha_4\beta_7$	148 ± 41 (50.8)	41 ± 5 (21.1)	52 ± 8 (22.9)	48 ± 3 (12.3)
CD44	1,574 ± 119 (99.2)	1,776 ± 266 (99.0)	2,269 ± 289 (99.7)	4,120 ± 535 (99.9)
CD54	1,234 ± 317 (99.2)	2,347 ± 227 (99.2)	2,371 ± 562 (99.9)	3,863 ± 283 (97.9)
CD103 (α_{IEL})	41 ± 11 (15.6)	25 ± 2 (6.2)	127 ± 32 (48.1)	40 ± 7 (9.3)
CD62L (L-selectin)	297 ± 74 (50.1)	37 ± 9 (28.7)	173 ± 44 (36.3)	73 ± 15 (41.4)
CD162 (PSGL-1)	2,812 ± 543 (98.8)	2,123 ± 103 (99.2)	4,406 ± 837 (99.7)	2,503 ± 9 (100)
P-selectin ligand	1,722 ± 414 (69.3)	888 (52.9)	4,363 ± 672 (73.9)	4,556 (90.4)
CCL19 receptor (CCR7)	655 ± 292 (31.4)	1,679 ± 128 (87.9)	1,983 ± 746 (56.7)	4,324 ± 461 (63.2)
CXCR4	186 (99)	554 (99)	252 (99)	550 (99)
Activation marker				
MHC class II	1,101 ± 270 (76.0)	1,645 ± 5 (94.9)	1,500 ± 307 (95.7)	1,705 ± 90 (80.1)
CD80	80 ± 20 (45.3)	1,816 ± 384 (91.8)	133 ± 32 (78.4)	2,326 ± 711 (77.6)
CD86	93 ± 30 (37.9)	2,138 ± 398 (95.0)	153 ± 42 (70.9)	3,575 ± 897 (83.8)
CD40	66 ± 18 (35.2)	654 ± 20 (87.9)	112 ± 31 (60.9)	693 ± 11 (73.5)

Expression is presented as mean fluorescence intensity ± s.e.m. where indicated as well as percentage of cells above background (in parentheses below); $n = 1$–7/group.
[a]The α_L integrin chain forms an obligate heterodimer (LFA-1) exclusively with the β_2 integrin chain; hence, α_L expression must reflect $\alpha_L\beta_2$ (LFA-1) expression.
[b]The α_4 integrin chain forms an obligate heterodimer with either β_1 (VLA-4) or β_7; therefore, α_4 on the surface represents the sum of $\alpha_4\beta_1$ (VLA-4) and $\alpha_4\beta_7$ heterodimers.

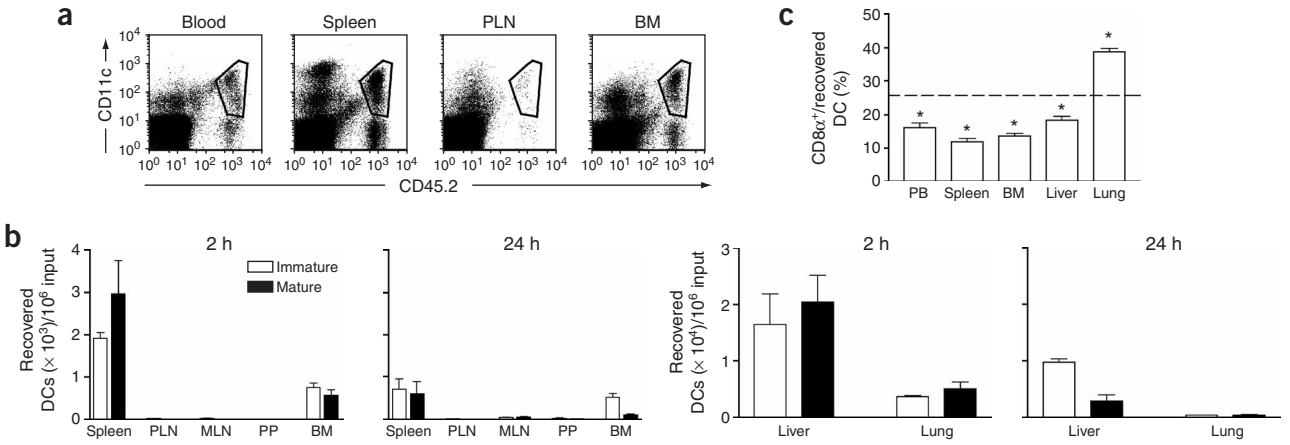

Figure 1 *In vivo* migration pathways of immature and mature DCs. (**a**) DC-enriched CD45.2$^+$ splenocyte samples were injected intravenously into CD45.1$^+$ mice and were allowed to circulate for 2 h. Donor DCs that had homed to recipient organs were identified by coexpression of CD45.2 and CD11c (outlined areas). (**b**) Organ distribution of freshly prepared, CFSE-labeled immature or LPS-matured DCs after intravenous injection. Recipient mice were injected with tagged DCs and organs were collected after 2 h or 24 h. The absolute number of DCs that had homed to each tissue was calculated by multiplication of the frequency of CD11c$^+$ transferred cells by the total number of resident leukocytes. Data are presented as number of recovered DCs per 1×10^6 injected. (**c**) Homing of CD8α$^+$CD11c$^+$ DCs (compared with total CD11c$^+$ DCs) to various organs after intravenous injection. Horizontal dashed line indicates the percentage of CD8α$^+$CD11c$^+$ DCs in the input sample. *, $P < 0.01$, $n = 4$–8/group. PLN, peripheral lymph node; BM, bone marrow; MLN, mesenteric lymph node; PP, Peyer's patches.

marrow corresponded to about 50% and about 20% of the respective splenic subset. Compared with that early time point, most mature DCs (88%) disappeared from the bone marrow at 24 h after injection, while the number of immature DCs decreased by only 39%. In contrast, immature DCs were rapidly cleared from the spleen (64% reduction).

Circulating DCs were almost completely excluded from all secondary lymphoid organs other than the spleen. This was consistent with the finding that neither immature nor mature DCs coexpressed sufficient L-selectin and CCR7 (**Table 1**), the prerequisite trafficking molecules for homing of lymphocytes to lymph nodes and Peyer's patches[16]. We noted equivalent patterns of DC distribution when we injected nonfluorescent CD45.2$^+$ DCs intravenously into congenic CD45.1$^+$ recipients (**Fig. 1a**) and when we obtained DCs from donors without Flt3 ligand–secreting tumors (data not shown), indicating that DC trafficking was not affected by the labeling procedure or by cytokine-induced expansion. Adoptive transfer of DCs (C57BL/6) into allogeneic (BALB/c or FVB) recipients yielded similar results (data not shown), indicating that DC recruitment was independent of the recipient's genetic background.

Subset-specific recruitment of circulating DCs

Differential expression of CD8α identifies discrete DC subsets with distinct migratory and functional properties as well as tissue distribution[17]. Thus, we sought to determine whether there were subset-specific differences in trafficking after intravenous injection. At 2 h after transfer of input cells comprising about 25% CD8α$^+$ DCs, the frequency of this subset among donor DCs was lower in peripheral blood and in all nonpulmonary recipient organs analyzed (**Fig. 1c**). Conversely, CD8α$^+$ DCs represented 38% of donor-derived DCs in the lung, suggesting that these relatively large cells are preferentially trapped in pulmonary capillaries. However, the ratio of CD8α$^+$ to CD8α$^-$ DCs in nonpulmonary sites, including the bone marrow, was similar to their ratio in blood, suggesting that CD8α$^+$ and CD8α$^-$ DC subsets migrate equivalently once they have passed the pulmonary 'sieve'. These experiments suggested that DC recruitment to noninflamed peripheral organs other than the lung is governed by tissue-specific factors regardless of the DC maturation state or subset membership. However, the retention and/or survival of DCs depends on their maturation state and the tissue environment, which seems especially favorable for immature DCs in the bone marrow.

DCs reach the bone marrow from peripheral tissues

Having determined that circulating DCs have bone marrow tropism, we sought to determine whether DCs can reach the bone marrow from peripheral sites. Thus, we labeled immature DCs with carboxyfluorescein succinimidyl ester (CFSE), deposited 2×10^6 to 8×10^6 of the DCs in both footpads and monitored their appearance in the draining popliteal lymph nodes, blood, spleen and bone marrow. When DC maturation was induced by simultaneous injection of 10 ng LPS, large numbers of DCs migrated to the popliteal lymph nodes, but even without LPS, a few DCs appeared within 24 h in the popliteal lymph nodes, and this population increased considerably at 48 h (**Fig. 2a**,**b**). The transferred immature DCs were almost undetectable in blood, spleen and bone marrow after 24 h. However, labeled DCs were readily recoverable from all three tissues at 48 h. Maturation accelerated DC dissemination from the footpad, as we recovered substantial numbers from blood, bone marrow and spleen as early as 24 h after injection.

Constitutive trafficking via blood to bone marrow

As immature DCs are present in normal peripheral blood[18], we sought to determine whether these endogenous DCs migrate to the bone marrow. We surgically joined CD45.1$^+$ and CD45.2$^+$ congenic mice at the flanks, which results in a shared circulation within 3 d. We then screened the bone marrow of parabiotic mice for partner-derived leukocytes[19].

We collected bone marrow 3–15 d after surgery, and in one experiment we separated mice 28 d after parabiosis and analyzed bone marrow 28 d later. As soon as a shared circulation was established, partner-derived leukocytes appeared in the bone marrow of these parabiotic mice (**Fig. 2c**). At 5 d after surgery, 1% and 1.9% of

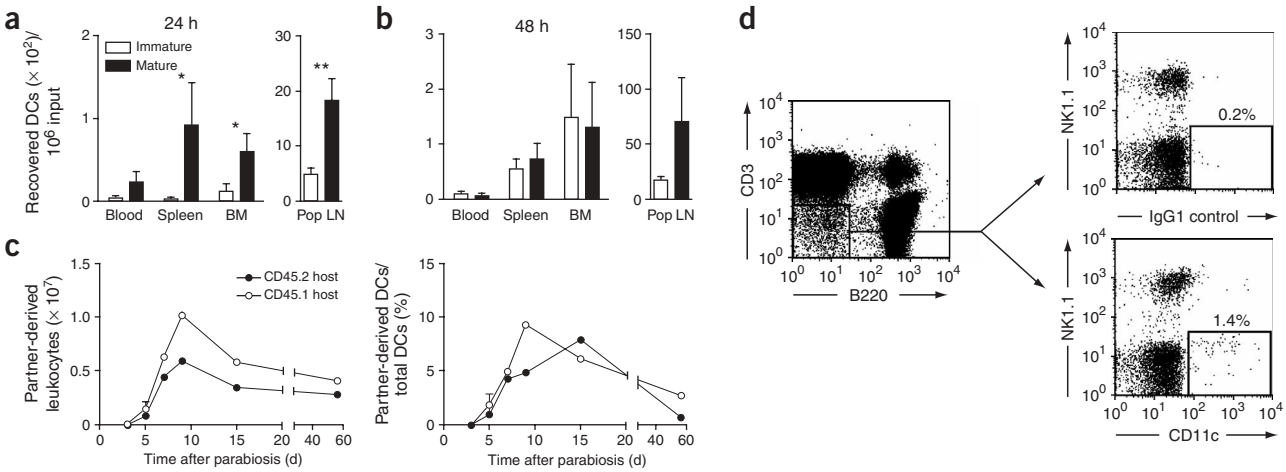

Figure 2 DCs traffic constitutively to bone marrow. Partially purified DCs were labeled with CFSE and injected in the footpads of recipient mice with (Mature) or without (Immature) LPS. After 24 h (**a**) or 48 h (**b**), blood, bone marrow and lymphoid organs were collected and the number of $CFSE^+$ DCs was determined. *, $P < 0.05$, **, $P < 0.01$, $n = 4$–6/group. PopLN, popliteal lymph node. (**c**) $CD45.1^+$ and $CD45.2^+$ mice were subjected to parabiosis and bone marrow was collected at various times after surgery. Left, time course of appearance of partner-derived leukocytes in the bone marrow of $CD45.2^+$ or $CD45.1^+$ parabiotic partners. Right, time course of appearance of partner-derived DCs in bone marrow ($n = 2$ mice/group at 3 and 5 d and 1 mouse/group at other times). (**d**) Representative flow cytometry showing small numbers of $NK1.1^-CD11c^+$ DCs (right, boxed areas with numbers above indicating frequency among nonlymphoid cells) contained in the $CD3^-B220^-$ leukocyte fraction (left, boxed area) in thoracic duct lymph.

DCs in the bone marrow were partner derived in CD45.2 and CD45.1 hosts, respectively (**Fig. 2c**). By day 15, the average frequency of bone marrow–resident partner-derived DCs was 7%. Consistent with the short lifespan of DCs[20], partner-derived DCs persisted poorly after separation. Nonetheless, it is likely that at later time points some of the partner-derived $CD11c^+$ arose from precursor cells that had homed to the bone marrow[19]. However, the rapid kinetics with which DCs became detectable after parabiosis indicate that full-fledged DCs migrate constitutively to normal bone marrow.

Thoracic duct lymph contains DCs

Having determined that a stream of circulating endogenous DCs enters the bone marrow, we sought to determine whether tissue-resident DCs also enter the bone marrow. Such peripheral DCs might enter draining lymphatics and bypass or traverse 'downstream' lymph nodes to reach the circulation via the thoracic duct. Indeed, thoracic duct lymph fluid from normal mice contained a small population of $NK1.1^-CD11c^+$ cells that constituted 0.013% ± 0.004% of viable cells (**Fig. 2d**), suggesting that a subtle, but continuous stream of DCs migrates from peripheral tissues through the lymph to the blood and from there to selected targets, including the bone marrow.

Molecular mechanisms of DC recruitment to bone marrow

Using intravital microscopy of mouse skull bone marrow[21], we characterized the molecules that enable blood-borne DCs to adhere to bone marrow microvessels. Both immature and mature DCs engaged in rolling in bone marrow venules and sinusoids (**Fig. 3a**), but immature DCs rolled more frequently than mature DCs (25.2% ± 1.4% versus 15.3% ± 1.3%, respectively; $P < 0.05$). There was no difference in the frequency with which rolling cells arrested (**Fig. 3b**). Injection of antibody to P-selectin (anti-P-selectin) reduced DC rolling by more than 50%. Even more inhibition was achieved with combined anti-P-selectin and anti-E-selectin, although anti-E-selectin alone was ineffective (**Fig. 3c**).

VCAM-1 is constitutively expressed in bone marrow microvessels and mediates firm adherence of hematopoietic progenitors in skull bone marrow[21]. The main ligand for VCAM-1, the integrin $\alpha_4\beta_1$ (VLA-4), is expressed on immature and mature DCs (**Table 1**). DC

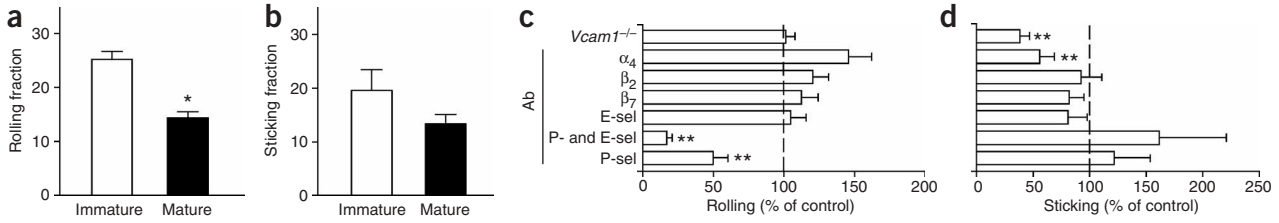

Figure 3 Molecular mechanism of the homing of DCs to bone marrow. $CD11c^+$ immature or mature DCs were labeled with calcein and were injected into the right carotid arteries of anesthetized mice. Interactions of injected cells with skull bone marrow microvessels were analyzed by epifluorescence intravital microscopy[21]. (**a**) Rolling fraction (percentage of rolling cells in the total flux of cells passing through a vessel) of immature or LPS-matured DCs. (**b**) Sticking fraction (percentage of rolling cells that arrested for 30 s or more) of immature and mature DCs. (**c**,**d**) Intravital microscopy of VCAM-1-deficient ($Vcam1^{-/-}$) or wild-type mice before and after monoclonal antibody treatment to characterize the adhesion pathways involved in the rolling (**c**) and sticking (**d**) of DCs in bone marrow microvessels. Results after monoclonal antibody treatment were normalized to those obtained with the same vessel before the treatment. Rolling and sticking fractions in VCAM-1-deficient mice were normalized to those of wild-type littermates. Ab, monoclonal antibody; E-sel, E-selectin; P-sel, P-selectin. *, $P < 0.05$, **, $P < 0.01$).

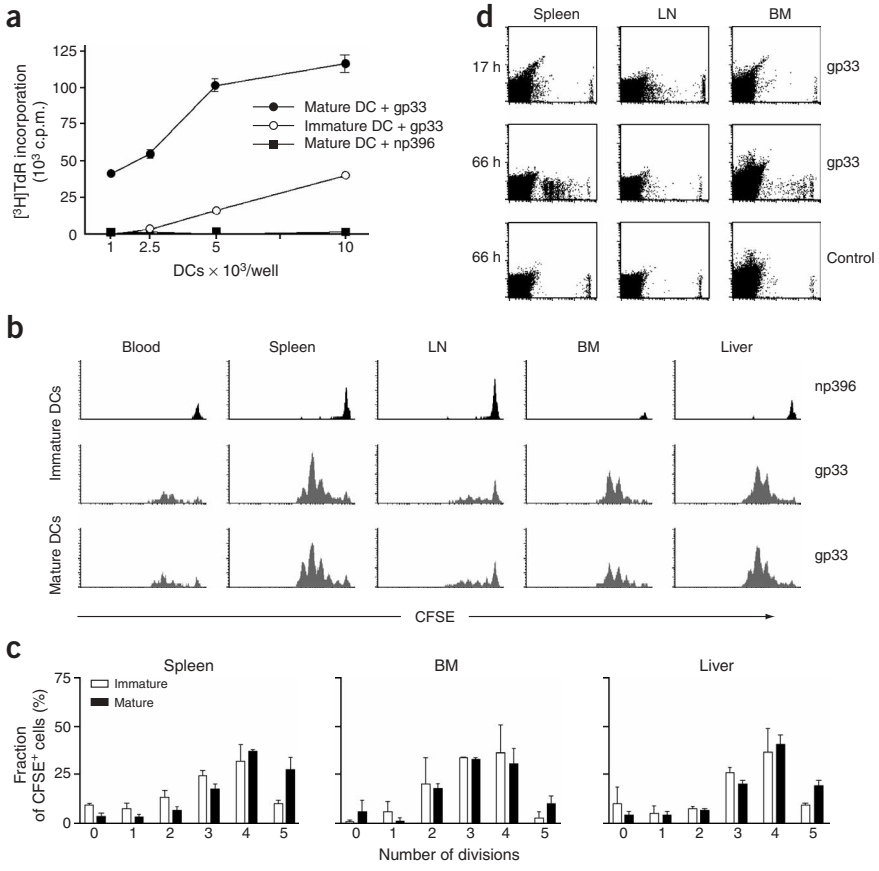

Figure 4 DCs that have homed induce antigen-specific T_{CM} cell proliferation in the bone marrow. (**a**) *In vitro* proliferation of T_{CM} cells in response to peptide-pulsed immature and mature DCs. Proliferation of T_{CM} cells in response to various numbers of gp33-pulsed mature or immature DCs (+ gp33) or np396-pulsed control DCs (+ np396) was measured by [^{3}H]thymidine ([^{3}H]TdR) incorporation after 3 d of coculture. (**b**) *In vivo* proliferation of CFSE-labeled T_{CM} cells 42 h after injection of immature DCs pulsed with gp33 or np396, or mature DCs pulsed with gp33. Histograms are gated on $V_\alpha2^+CFSE^+$ cells. (**c**) T cell proliferation in spleen, bone marrow and liver induced by immature DCs and mature DCs (n = 2–4/group). (**d**) Flow cytometry of T_{CM} cell proliferation. Mice containing CFSE-labeled T_{CM} cells were injected with mature gp33-pulsed or control DCs. Spleen, bone marrow and lymph nodes were removed 17 h later and single-cell suspensions were cultured for 2 more days (66 h). Cultures contained single-cell suspensions prepared from tissues without any addition of cytokines.

sticking was significantly reduced by treatment with antibody to the α_4 integrin chain and in VCAM-1-deficient mice ($P < 0.01$; **Fig 3d**). Thus, circulating DCs interact with the two endothelial selectins to roll and with VCAM-1 to arrest in normal bone marrow microvessels. Notably, although firm arrest on VCAM-1 presumably required that the rolling DCs receive a chemoattractant signal that activates $\alpha_4\beta_1$, DC sticking was unaffected after $G\alpha_i$ protein blockade with pertussis toxin (data not shown). Moreover, DC sticking was not reduced by antibody to the integrin $\alpha_L\beta_2$ (LFA-1), which mediates leukocyte arrest in other microvascular beds[16] and is abundantly expressed on DCs (**Table 1**). The recruitment signals for bone marrow–tropic DCs are thus very similar to the multistep adhesion cascade that mediates homing of hematopoietic progenitors and T_{CM} cells to the bone marrow[12,21].

DCs can activate bone marrow–resident T_{CM} cells

To determine whether blood-borne DCs could trigger immune responses after homing to the bone marrow, we intravenously injected CFSE-labeled DCs and then sorted them from recipient organs 24 h later. Recovered DCs from bone marrow and spleen were as potent as freshly isolated splenic DCs at stimulating allogeneic T cells (data not shown). Thus, homing does not alter the immunostimulatory capacity of DCs. Next we sought to determine whether DCs can transport and present antigen to T_{CM} cells, which represent the principal subset among human and mouse bone marrow–resident T cells[12]. We obtained $CD8^+$ T cells from mice carrying the P14 TCR transgene and differentiated the TCR-transgenic $CD8^+$ T cells into T_{CM}-like cells using established tissue culture methods[22]. T_{CM} cells differentiated *in vitro* have homing characteristics equivalent to those of endogenous T_{CM} cells[23], migrate avidly to the bone marrow[12] and are readily restimulated by recall antigen[22]. Accordingly, P14 T_{CM} cells proliferated vigorously during coculture with mature and, to a lesser extent, immature DCs that had been pulsed with specific peptide antigen (lymphocytic choriomeningitis glycoprotein 33–41 (gp33)) but not those pulsed with irrelevant peptide antigen (lymphocytic choriomeningitis nucleoprotein 396–404 (np396)) (**Fig. 4a**).

To determine whether DCs could also stimulate bone marrow–resident T_{CM} cells *in vivo*, we injected 5×10^6 to 7×10^6 CFSE-labeled P14 T_{CM} cells intravenously into recipient mice, then allowed the mice to 'rest' for 24 h. We then intravenously injected 3×10^6 to 5×10^6 immature or mature DCs pulsed with gp33 or control peptide. Then, 2 d later, we collected T_{CM} cells from various organs and analyzed them for CFSE dilution, a measure of proliferation. As expected, T cells did not divide in mice injected with np396-pulsed DCs (**Fig. 4b**), whereas gp33-pulsed DCs elicited vigorous T cell proliferation in spleen, liver and bone marrow (**Fig. 4c**). By 42 h after mature DC injection, T_{CM} cells had divided four to five times in these organs; in recipients of immature DCs, T_{CM} cells had also divided, but their division lagged behind that of cells stimulated with mature DCs by about half a division. Regardless of the maturation state of the injected DCs, few T_{CM} cells proliferated in lymph nodes, which is consistent with the inability of circulating DCs to home to these organs[24].

To exclude the possibility that the divided T_{CM} cells found in DC-challenged bone marrow had homed there after having received activation signals elsewhere, we collected organs early (17 h) after DC injection, before any T_{CM} cells had a chance to divide (**Fig. 4d**). We then maintained single-cell suspensions of collected tissues *in vitro*. After 2 d in culture, vigorous T cell proliferation was apparent in both spleen and bone marrow cultures from recipients of gp33-pulsed DCs. This effect was antigen specific, as tissue cultures from mice that had received control peptide–pulsed DCs contained only undivided T_{CM} cells. Lymph node cultures from recipients of gp33-pulsed DCs showed no T_{CM} cell proliferation, suggesting that the few divided cells in lymph nodes collected 42 h after DC injection had been

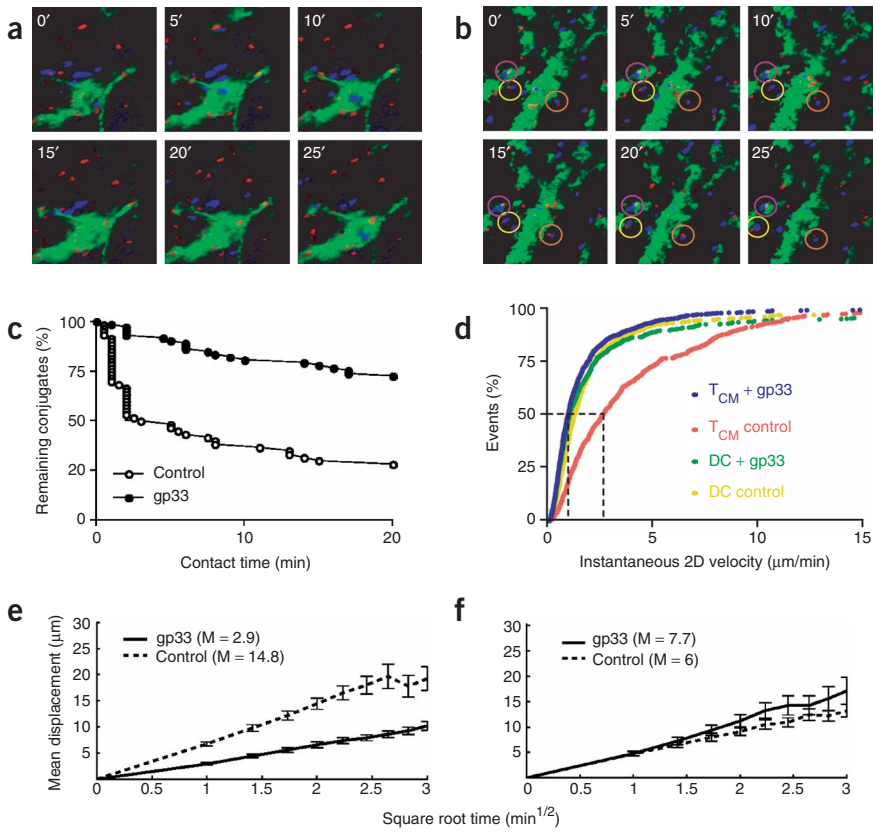

Figure 5 Two-photon microscopy analysis of T_{CM} cell–DC interactions and motility in skull bone marrow. (**a**,**b**) Intravital multiphoton micrographs of a bone marrow cavity in a mouse skull after injection of T_{CM} cells (blue) and mature DCs (red) that were unpulsed (**a**) or were pulsed with gp33 peptide (**b**). Vessels were delineated by injection of fluorescein isothiocyanate–dextran (green; 2 MDa). Time-lapse images at 5-minute intervals (top left corners; ′, min) illustrate contacts between T_{CM} cells and DCs in the absence or presence of antigen. Colored circles indicate three representative stable conjugates. (**c**) Duration of T cell–DC conjugates with (gp33) or without (Control) gp33 antigen, presented as cumulative dissociation curves. (**d**) Instantaneous two-dimensional (2D) velocities for individual DCs and T_{CM} cells, determined with automatic tracking software and presented as cumulative velocity curves. *, $P < 0.001$, T_{CM} cell control (red) versus T_{CM} cell plus gp33 (blue), Mann-Whitney *U*-test for nongaussian distributions. (**e**,**f**) Mean displacement plots for T_{CM} cells (**e**) and DCs (**f**) in the presence (gp33) or absence (Control) of antigen. The motility coefficient (M) for each population is in parentheses.

stimulated elsewhere and subsequently migrated to lymph nodes through the blood. Conversely, T_{CM} cell proliferation in early bone marrow cultures demonstrated that bone marrow–tropic DCs are immunocompetent. Thus, at least a fraction of the divided T_{CM} cells found in bone marrow *in vivo* (**Fig. 4b**) was most likely activated by DCs that had homed *in situ*.

Visualization of T cell–DC interactions in bone marrow

Having determined that circulating DCs can carry antigen to the bone marrow and potently stimulate antigen-specific responses by T_{CM} cells, we sought to determine whether and how DCs and T_{CM} cells interact in the bone marrow. For this, we used two-photon intravital microscopy of mouse skull bone marrow cavities[12] (**Fig. 5a**,**b**). We labeled P14 T_{CM} cells with the blue nuclear dye Hoechst 33342 and injected them intravenously into recipient mice. We labeled peptide-pulsed DCs with CMTMR, a red-orange fluorophor, and injected them 12–16 h later. After 2 h, we prepared the mice for two-photon intravital microscopy as described[12]. We visualized the luminal compartment of bone marrow microvessels with fluorescein isothiocyanate–dextran and acquired three-color fluorescence image stacks over 30 min (1 stack/min) to record three-dimensional time-lapse videos of extravascular T_{CM} cell–DC interactions.

With no antigen present, both DCs and T_{CM} cells showed continuous random movements throughout the bone marrow cavity (**Supplementary Video 1** online), and most contacts between DCs and T_{CM} cells were brief, although about one in four T_{CM} cells remained associated with DCs throughout the observation period (**Fig. 5c**). However, most antigen-independent prolonged contacts were not associated with a change in the shape of the T cells, whereas P14 T_{CM} cells polarized to undergo tight, long-lasting contacts with a broadened interface with gp33-pulsed DCs (**Fig. 5b**,**c** and **Supplementary Video 2** online). The presence of antigen also resulted in a decrease in T_{CM} cell instantaneous velocity, whereas DCs migrated slowly whether they presented cognate antigen to T_{CM} cells or not (**Fig. 5d**). This was also reflected in the mean square displacement plots (a measure of cell motility[25]), which showed a notable antigen-dependent suppression in the motility of T_{CM} cells (**Fig. 5e**) but not of DCs (**Fig. 5f**).

DISCUSSION

We conceived this study with the objective of better defining the target organs of circulating DCs. It is already well established that tissue-resident DCs continuously sample antigen in peripheral tissues and carry it to draining lymph nodes, where they present it to recirculating T cells[1]. A small fraction of DCs from certain peripheral tissues can relocate to distant secondary lymphoid organs that are not connected by lymphatics, indicating that some tissue-resident DCs can return to the blood[5–7]. Those observations indicate that blood-borne DCs may be highly migratory and may comprise more than one subset distinguished by different histories and perhaps destined for distinct target tissues[18,26,27]. However, the present understanding of blood-borne DC trafficking is based mainly on comparisons of DC vaccines administered by different routes[8]. In addition, it is known that blood-borne DCs migrate to inflamed tissues[28], but the paths taken by circulating DCs in the absence of inflammation are still poorly understood.

Our initial strategy was to inject labeled primary DCs into mice to track their migration. However, the number of true DCs that can be routinely collected from normal mice is prohibitively small for *in vivo* trafficking studies. To overcome this obstacle, we implanted donor mice with a melanoma secreting Flt3 ligand, which substantially increased production of all DC subsets without perturbing their function[14,15]. When we intravenously injected purified DC populations expanded by Flt3 ligand, they migrated preferentially to the liver, lung and spleen but were excluded from all other secondary lymphoid organs, consistent with published observations[24,29–31]. The inability of

circulating DCs to home to lymph nodes and Peyer's patches is due to insufficient expression of essential homing receptors, especially L-selectin and, on immature DCs, CCR7 (ref. 24). In contrast, DCs have abundant expression of ligands for selectins and $\alpha_4\beta_1$, the VCAM-1 receptor[15,24]. Both endothelial selectins as well as VCAM-1 are constitutively expressed in bone marrow, where they mediate recruitment of hematopoietic progenitors and T_{CM} cells[12,21,32]. Indeed, homing of DCs to the bone marrow depended on rolling mediated by P-selectin (and E-selectin), followed by VCAM-1-dependent sticking. Notably, the number of DCs that homed to bone marrow was comparable to that in the spleen, and the bone marrow retained DCs even better than the spleen after 24 h.

One caveat was that the injection of supraphysiological numbers of DCs could have saturated the sites at which DCs normally exit the circulation, resulting in abnormal spillover to the bone marrow. Therefore, we studied DC migration in parabiotic mice. In these experiments, partner-derived DCs were detectable in the bone marrow with kinetics that were much more rapid than the slow differentiation of DCs from progenitors[26]. We conclude that substantial numbers of full-fledged DCs continuously access normal bone marrow from the blood.

What are the functional consequences of this migratory pathway? The bone marrow can function as a secondary lymphoid organ in virus-infected mice in which lymphocytes cannot traffic to secondary lymphoid organs[33]. Thus, the bone marrow provides a suitable microenvironment for T cell priming. Homing of immature DCs to the bone marrow could contribute to this function by supplying highly phagocytic cells that may collect antigen locally. Additionally, DCs can capture antigen in the blood and subsequently migrate to extravascular sites to prime lymphocytes[4].

Although the physiological function of the bone marrow during T cell priming is still being debated, there is mounting evidence that the bone marrow is involved in recall responses and memory T cell homeostasis[33]. Indeed, viral infections induce the formation of T_{CM} cells that are particularly important for long-term protection[34]. These cells preferentially accumulate and proliferate in the bone marrow and mount stronger effector responses than the corresponding population in the blood[33]. Moreover, evidence has suggested that optimal preservation of CD8 memory requires the presence of DCs[35]. Given those findings, we hypothesized that DCs could traffic to the bone marrow to trigger recall responses by bone marrow–resident T_{CM} cells.

As predicted, DCs that had homed efficiently to bone marrow stimulated bone marrow–resident T_{CM} cells. In contrast to results with naive T cells, which are only activated by mature DCs, T_{CM} cell proliferation was readily noted with immature DCs. This is consistent with the lower costimulation requirements for memory T cell activation than for naive T cells[9]. Another difference between naive T cells and T_{CM} cells was suggested by our two-photon microscopy experiments; as early as 2 h after DC injection, almost all T_{CM} cell–DC interactions were manifested as tight, long-lasting conjugates. In contrast, two-photon intravital microscopy of naive T cell priming with the same peptide antigen in lymph nodes showed that there was an initial phase of about 8 h during which T cells touched antigen-presenting DCs only briefly. Tight contacts were found only thereafter[36]. The faster kinetics of stable conjugation in the bone marrow might reflect the enhanced susceptibility of T_{CM} cells to recall antigen. Alternatively, the bone marrow microenvironment may foster T cell–antigen-presenting cell interaction kinetics different from those of peripheral lymph nodes.

An important issue was whether tissue-resident DCs can collect antigen and then migrate to the bone marrow through the blood. It seemed plausible that such peripheral DCs might enter local lymphatics and bypass or traverse 'downstream' lymph nodes to reach the circulation through the thoracic duct. Consistent with that idea, we found that thoracic duct lymph fluid in normal mice contained a small DC population that comprised 0.013% ± 0.004% viable cells. Assuming a leukocyte flux of about 7×10^6 cells/h through the thoracic duct of an adult mouse[37], we calculate that at least 2.2×10^4 peripheral DCs return to the circulation via this route every day. Only a fraction of this population is likely to migrate to the bone marrow, whereas our results in parabiotic mice indicated that at least 3×10^4 partner-derived DCs enter the bone marrow every day. Therefore, DCs can probably also reach the blood–bone marrow conduit via routes other than lymphatics.

Indeed, whereas the mechanisms that govern interstitial DC migration into draining lymph vessels are partially understood, it is unclear whether this is the only route by which DCs leave tissues. For example, high endothelial venules and chronically inflamed microvessels express CCL21, a ligand for CCR7, which mediates lymphocyte traffic in secondary lymphoid organs and is also required for DC migration into lymph vessels[38]. It is conceivable that $CCR7^+$ DCs could enter the bloodstream by migrating across $CCL21^+$ venules. Indeed, monocyte-derived DCs can undergo reverse transmigration, whereby they cross an endothelial monolayer from the extravascular compartment to the lumen[39].

The suggestion that tissue-resident DCs could reach the blood and then migrate to other organs has surfaced repeatedly in the literature but has not been addressed systematically. DCs carry fluorescent beads, dyes or antigens to the spleen after either intracutaneous injection or instillation into the lung[5–7,40,41]. Those cells could only reach the spleen by re-entering the circulation. Similarly, after solid organ transplantation, graft-derived DCs appear rapidly in the recipient's blood and spleen[42,43]. Finally, $CD18^+$ leukocytes, including $CD11c^+$ DCs, collect *Salmonella typhimurium* from the intestinal lumen and then appear in the blood as early as 15 min after intragastric infection[44]. We have done similar experiments by infecting mice orally with invasion-deficient *S. typhimurium*. At 30–60 min after infection, we detected small numbers (10–20 colony-forming units/ml) of bacteria in peripheral blood. By 24–36 h after infection, we were able to culture bacteria from the bone marrow (30–1,120 colony-forming units/whole bone marrow) and the spleen (150–9,700 colony-forming units/spleen). Indeed, using green fluorescent protein–tagged *S. typhimurium*, we detected green fluorescent protein–positive DCs in the spleen and bone marrow of infected mice (unpublished data).

Our results provide evidence for a migratory route that channels DCs from peripheral tissues. Whereas the number of DCs that could be recovered from the bone marrow was 3–10% of what was found in the draining lymph nodes, the relatively small number of migrating DCs might well be sufficient to elicit substantial immune responses by the highly reactive memory T cell population that is prevalent in the bone marrow. After deposition in the footpad, equivalent numbers of immature and mature DCs were recovered from the bone marrow, although the former migrated more slowly than the latter. This maturation-dependent difference in migratory kinetics indicated that the departure of DCs from peripheral tissues is an active process and is not simply a consequence of the sudden increase in interstitial pressure caused by cell injection.

Our findings demonstrate that small numbers of DCs continuously leave peripheral tissues and gain access to the bloodstream via the thoracic duct. Using adoptive transfer protocols and several approaches to trace endogenous DCs, we have shown that blood-borne mature and immature DCs home to normal bone marrow

through a multistep cascade that involves P-selectin and E-selectin as well as VCAM-1. Our experimental data suggest that DCs can take this previously unknown migration route to induce rapid antigen-specific activation of bone marrow–resident $CD8^+$ T_{CM} cells as a truly central memory response.

METHODS

Mice. C57BL/6 (CD45.2/Ly5.2), congenic CD45.1/Ly5.1 (B6.SJL-*Ptprc*^{a}*Pep3*^{b}/*BoyJ*), FVB and BALB/c mice were purchased from Jackson Labs, Taconic or Charles River Laboratories. P14 transgenic mice[45] were obtained from Jackson Labs. Mice with conditional deficiency of VCAM-1 in the endothelium were generated as described[46]. All mice were housed and bred in a specific pathogen–free and viral antibody–free animal facility. All experiments were done in accordance with National Institutes of Health guidelines and were approved by Committees on Animals at both Harvard Medical School and the CBR Institute (Boston, Massachusetts).

Reagents. The lymphocytic choriomeningitis virus gp33 (KAVYNFATC) and np396 (FQPQNGQFI) peptides were synthesized at Biosource International.

Antibodies. For intravital microscopy, monoclonal antibodies to P-selectin (clone 5H1) and E-selectin (9A9) were provided by B. Wolitzky (Hoffman LaRoche, Nutly, New Jersey); monoclonal antibodies to CD11a (TIB213) and the integrin chains α_4 (PS/2) and β_7 (FIB504) were a gift from E. Butcher (Stanford University, California). Monoclonal antibody to the integrin chain β_2 (GAME-46) was purchased from Pharmingen.

For flow cytometry, fluorochrome-labeled monoclonal antibodies were purchased from Pharmingen. Expression of P-selectin ligands was detected with P-selectin–immunoglobulin (Pharmingen). CCR7 expression was measured by the binding of CCL19-immunoglobulin[23]. Data were acquired with a FACSCalibur flow cytometer and were analyzed with CellQuest software (BD Biosciences).

Cell preparation. Splenic DCs were isolated from C57BL/6 mice injected subcutaneously 11–14 d before with 4×10^6 Flt3 ligand–secreting B16 tumor cells. For homing assays, total splenocyte samples were enriched for DCs by density gradient centrifugation over Optiprep (Sigma-Aldrich) and the low-density cells were collected. DC-enriched preparations routinely contained 75–85% $CD11c^+$ DCs. For intravital microscopy, $CD11c^+$ DCs were purified by positive selection with anti-CD11c microbeads (greater than 95% $CD11c^+$; Miltenyi Biotec). DC maturation was induced by culture for 24–48 h in the presence of 1 μg/ml of LPS (*E.coli* 0.26:B6; Sigma) or by simultaneous injection of 10 ng LPS/footpad. T_{CM} cells were generated *in vitro* using established techniques[22].

Homing assays. DCs were labeled for 20 min at 37° C with 30 μM CFSE (5(6)-carboxyfluorescein succinimidyl ester; Molecular Probes). Recipient mice were injected intravenously with 2×10^7 to 5×10^7 DCs. In some experiments, 2×10^6 to 8×10^6 DCs were injected subcutaneously into both footpads instead. After 2–48 h, recipient mice were killed and blood and other organs were collected and processed to single-cell suspensions. Livers and lungs were first digested with collagenase type 2 (0.5%; Worthington Biochemical). Bone marrow was collected from tibias and femora of hind legs, which accounts for about 20% of total body bone marrow[47]. Cells that had homed were identified as DCs by CD11c staining.

Cannulation of the thoracic duct. C57BL/6 mice were fed 700 μl of olive oil by gavage. Then, 45 min later, mice were anaesthetized by intraperitoneal injection of ketamine (50 mg/kg) and xylazine (10 mg/kg) and were subjected to laparotomy. A heparinized PE-10 polyethylene catheter was inserted into the cysterna chyli[48] and lymph was collected for 30–45 min, stained with monoclonal antibodies and analyzed by flow cytometry.

Intravital microscopy. Intravital microscopy of mouse cranial bone marrow microcirculation was done as described[21]. Boluses of DCs labeled with calcein–acetoxymethyl ester (Molecular Probes) were injected into the carotid artery in a retrograde direction. Cells that entered the bone marrow microvasculature were visualized by video-triggered stroboscopic epi-illumination (Chadwick Helmuth) through a fluorescein isothiocyanate filter set. Video images were recorded with a low-lag silicon-intensified target camera (VE1000-SIT; Dage MTI), a time-base generator (For-A) and a Hi8 VCR (Sony). Cell activity was determined by offline analysis. The rolling fraction per venule was measured as the percentage of DCs that interacted with the vascular wall of total fluorescent cells that passed through the vessel during the observation period. The sticking fraction was defined as the percentage of rolling cells that became firmly adherent for 30 s or more.

Parabiotic mice. Pairs of parabiotic mice consisting of one CD45.1 and one CD45.2 congenic mouse were prepared as described[19]. Pairs of mice were analyzed between 3 and 28 d after parabiosis. One pair of mice was surgically separated after 28 d and was analyzed 28 d later.

***In vivo* antigen presentation.** Mice were injected intravenously with 5×10^6 to 7×10^6 CFSE-labeled P14 T_{CM} cells. Then, 24 h later, the same mice were injected intravenously with 3×10^6 to 5×10^6 peptide-pulsed DCs (5 μg/ml for 2 h at 37 °C). After a further 42–48 h, organs were collected and single-cell suspensions were stained for the P14-specific TCR $V_\alpha 2$. In some experiments, mice were killed 17–18 h after DC injection, organs were collected and unpurified single-cell suspensions were cultured without additional cytokines for up to 3 d. Proliferation was assessed by CFSE dilution as described[49].

Two-photon microscopy. For two-photon imaging, P14 T_{CM} cells were labeled for 20 min at 37 °C with Hoechst 33342 (10 μg/ml; Molecular Probes) before intravenous injection into recipient mice. Then, 16–18 h later, mice were injected intravenously with DCs labeled with 10 μM CMTMR (5-and-6, 4-chloromethylbenzoylamino tetramethylrhodamine; Molecular Probes). Imaging began approximately 2–3 h after injection of DCs. Mice were prepared for intravital microscopy imaging of the skull bone marrow as described[12]. Immediately before imaging, mice were injected with fluorescein isothiocyanate–dextran (2 MDa; Sigma) to visualize bone marrow vasculature. Two-photon imaging was done with an Olympus BX50WI fluorescence microscope equipped with a 20× objective with a numerical aperture of 0.95 and a Radiance 2100MP Confocal/Multiphoton microscopy system, controlled by Lasersharp software (BioRad). For two-photon excitation, a MaiTai Broadband Ti:S laser (Spectra Physics) was tuned to 800 nm.

Three-dimensional analysis of cell migration has been described[12,36]. Stacks of *x-y* sections were acquired every 30–60 s. Sequences of image stacks were transformed into volume-rendered four-dimensional movies with Volocity software (Improvision), which was also used for semiautomated tracking of moving objects. From centroid coordinates, parameters of cellular motility were calculated with custom scripts in Matlab (MathWorks)[50].

Statistical analysis. All data are presented as mean ± s.e.m. Students' *t*-test was used for comparisons of two groups. In all cases, *P* values of less than 0.05 were considered statistically significant.

Note: Supplementary information is available on the Nature Immunology website.

ACKNOWLEDGMENTS

We thank A. Vazquez-Torres (University of Colorado) for mutant strains of salmonella; G. Cheng and B. Reinhardt for technical support; and L. Scimone for help with intravital microscopy analysis. Supported by National Institutes of Health (AI061663, HL62524, HL54936 and HL56949 to U.H.v.A.); an Amy Potter fellowship, the Charles Hood Foundation and the Multiple Myeloma Foundation (I.B.M.); and Federazione Italiana Ricerca sul Cancro (R.B.).

COMPETING INTERESTS STATEMENT

The authors declare that they have no competing financial interests.

Published online at http://www.nature.com/natureimmunology/
Reprints and permissions information is available online at http://npg.nature.com/reprintsandpermissions/

1. Banchereau, J. *et al.* Immunobiology of dendritic cells. *Annu. Rev. Immunol.* **18**, 767–811 (2000).
2. Cavanagh, L.L. & von Andrian, U.H. Travellers in many guises: The origins and destinations of dendritic cells. *Immunol. Cell Biol.* **80**, 448–462 (2002).
3. Sallusto, F. *et al.* Rapid and coordinated switch in chemokine receptor expression during dendritic cell maturation. *Eur. J. Immunol.* **28**, 2760–2769 (1998).

4. Balazs, M., Martin, F., Zhou, T. & Kearney, J. Blood dendritic cells interact with splenic marginal zone B cells to initiate T-independent immune responses. *Immunity* **17**, 341–352 (2002).
5. Randolph, G.J., Inaba, K., Robbiani, D.F., Steinman, R.M. & Muller, W.A. Differentiation of phagocytic monocytes into lymph node dendritic cells in vivo. *Immunity* **11**, 753–761 (1999).
6. Legge, K.L. & Braciale, T.J. Accelerated migration of respiratory dendritic cells to the regional lymph nodes is limited to the early phase of pulmonary infection. *Immunity* **18**, 265–277 (2003).
7. Mullins, D.W. *et al.* Route of immunization with peptide-pulsed dendritic cells controls the distribution of memory and effector T cells in lymphoid tissues and determines the pattern of regional tumor control. *J. Exp. Med.* **198**, 1023–1034 (2003).
8. Schuler, G., Schuler-Thurner, B. & Steinman, R.M. The use of dendritic cells in cancer immunotherapy. *Curr. Opin. Immunol.* **15**, 138–147 (2003).
9. Sallusto, F., Geginat, J. & Lanzavecchia, A. Central memory and effector memory T cell subsets: function, generation, and maintenance. *Annu. Rev. Immunol.* **22**, 745–763 (2004).
10. Di Rosa, F. & Santoni, A. Bone marrow CD8 T cells are in a different activation state than those in lymphoid periphery. *Eur. J. Immunol.* **32**, 1873–1880 (2002).
11. Becker, T.C., Coley, S.M., Wherry, E.J. & Ahmed, R. Bone marrow is a preferred site for homeostatic proliferation of memory CD8 T cells. *J. Immunol.* **174**, 1269–1273 (2005).
12. Mazo, I.B. *et al.* Bone marrow is a major reservoir and site of recruitment for central memory CD8$^+$ T cells. *Immunity* **22**, 259–270 (2005).
13. Feuerer, M. *et al.* Therapy of human tumors in NOD/SCID mice with patient-derived reactivated memory T cells from bone marrow. *Nat. Med.* **7**, 452–458 (2001).
14. Maraskovsky, E. *et al.* Dramatic increase in the numbers of functionally mature dendritic cells in Flt3 ligand-treated mice: multiple dendritic cell subpopulations identified. *J. Exp. Med.* **184**, 1953–1962 (1996).
15. Mora, J.R. *et al.* Selective imprinting of gut-homing T cells by Peyer's patch dendritic cells. *Nature* **424**, 88–93 (2003).
16. von Andrian, U.H. & Mackay, C.R. T-cell function and migration. Two sides of the same coin. *N. Engl. J. Med.* **343**, 1020–1034 (2000).
17. Shortman, K. & Liu, Y.J. Mouse and human dendritic cell subtypes. *Nat. Rev. Immunol.* **2**, 151–161 (2002).
18. Donnenberg, V.S. *et al.* Rare-event analysis of circulating human dendritic cell subsets and their presumptive mouse counterparts. *Transplantation* **72**, 1946–1951 (2001).
19. Wright, D.E., Wagers, A.J., Gulati, A.P., Johnson, F.L. & Weissman, I.L. Physiological migration of hematopoietic stem and progenitor cells. *Science* **294**, 1933–1936 (2001).
20. Kamath, A.T. *et al.* The development, maturation, and turnover rate of mouse spleen dendritic cell populations. *J. Immunol.* **165**, 6762–6770 (2000).
21. Mazo, I.B. *et al.* Hematopoietic progenitor cell rolling in bone marrow microvessels: Parallel contributions by endothelial selectins and VCAM-1. *J. Exp. Med.* **188**, 465–474 (1998).
22. Manjunath, N. *et al.* Effector differentiation is not prerequisite for generation of memory cytotoxic T lymphocytes. *J. Clin. Invest.* **108**, 871–878 (2001).
23. Weninger, W., Crowley, M.A., Manjunath, N. & von Andrian, U.H. Migratory properties of naive, effector, and memory CD8$^+$ T cells. *J. Exp. Med.* **194**, 953–966 (2001).
24. Robert, C. *et al.* Gene therapy to target dendritic cells from blood to lymph nodes. *Gene Ther.* **10**, 1479–1486 (2003).
25. Sumen, C., Mempel, T.R., Mazo, I.B. & von Andrian, U.H. Intravital microscopy; visualizing immunity in context. *Immunity* **21**, 315–329 (2004).
26. del Hoyo, G.M. *et al.* Characterization of a common precursor population for dendritic cells. *Nature* **415**, 1043–1047 (2002).
27. O'Keeffe, M. *et al.* Dendritic cell precursor populations of mouse blood: identification of the murine homologues of human blood plasmacytoid pre-DC2 and CD11c$^+$ DC1 precursors. *Blood* **101**, 1453–1459 (2003).
28. Robert, C. *et al.* Interaction of dendritic cells with skin endothelium: A new perspective on immunosurveillance. *J. Exp. Med.* **189**, 627–636 (1999).
29. Fossum, S. Lymph-borne dendritic leucocytes do not recirculate, but enter the lymph node paracortex to become interdigitating cells. *Scand. J. Immunol.* **27**, 97–105 (1988).
30. Kupiec-Weglinski, J.W., Austyn, J.M. & Morris, P.J. Migration patterns of dendritic cells in the mouse. Traffic from the blood, and T cell-dependent and -independent entry to lymphoid tissues. *J. Exp. Med.* **167**, 632–645 (1988).
31. Lappin, M.B. *et al.* Analysis of mouse dendritic cell migration in vivo upon subcutaneous and intravenous injection. *Immunology* **98**, 181–188 (1999).
32. Frenette, P.S., Subbarao, S., Mazo, I.B., von Andrian, U.H. & Wagner, D.D. Endothelial selectins and vascular cell adhesion molecule-1 promote hematopoietic progenitor homing to bone marrow. *Proc. Natl. Acad. Sci. USA* **95**, 14423–14428 (1998).
33. Di Rosa, F. & Pabst, R. The bone marrow: a nest for migratory memory T cells. *Trends Immunol.* **26**, 360–366 (2005).
34. Wherry, E.J. *et al.* Lineage relationship and protective immunity of memory CD8 T cell subsets. *Nat. Immunol.* **4**, 225–234 (2003).
35. Zammit, D.J., Cauley, L.S., Pham, Q.M. & Lefrancois, L. Dendritic cells maximize the memory CD8 T cell response to infection. *Immunity* **22**, 561–570 (2005).
36. Mempel, T.R., Henrickson, S.E. & von Andrian, U.H. T cell priming by dendritic cells in lymph nodes occurs in three distinct phases. *Nature* **427**, 154–159 (2004).
37. Gesner, B.M. & Gowans, J.L. The output of lymphocytes from the thoracic duct of unanaesthetized mice. *Br. J. Exp. Path.* **43**, 424–430 (1962).
38. von Andrian, U.H. & Mempel, T.R. Homing and cellular traffic in lymph nodes. *Nat. Rev. Immunol.* **3**, 867–878 (2003).
39. Randolph, G.J., Beaulieu, S., Lebecque, S., Steinman, R.M. & Muller, W.A. Differentiation of monocytes into dendritic cells in a model of transendothelial trafficking. *Science* **282**, 480–483 (1998).
40. Enioutina, E.Y., Visic, D. & Daynes, R.A. The induction of systemic and mucosal immune responses to antigen-adjuvant compositions administered into the skin: alterations in the migratory properties of dendritic cells appears to be important for stimulating mucosal immunity. *Vaccine* **18**, 2753–2767 (2000).
41. Racanelli, V., Behrens, S.E., Aliberti, J. & Rehermann, B. Dendritic cells transfected with cytopathic self-replicating RNA induce crosspriming of CD8$^+$ T cells and antiviral immunity. *Immunity* **20**, 47–58 (2004).
42. Larsen, C.P., Morris, P.J. & Austyn, J.M. Migration of dendritic leukocytes from cardiac allografts into host spleens. A novel pathway for initiation of rejection. *J. Exp. Med.* **171**, 307–314 (1990).
43. Saiki, T., Ezaki, T., Ogawa, M. & Matsuno, K. Trafficking of host- and donor-derived dendritic cells in rat cardiac transplantation: allosensitization in the spleen and hepatic nodes. *Transplantation* **71**, 1806–1815 (2001).
44. Vazquez-Torres, A. *et al.* Extraintestinal dissemination of Salmonella by CD18-expressing phagocytes. *Nature* **401**, 804–808 (1999).
45. Pircher, H., Burki, K., Lang, R., Hengartner, H. & Zinkernagel, R.M. Tolerance induction in double specific T-cell receptor transgenic mice varies with antigen. *Nature* **342**, 559–561 (1989).
46. Koni, P.A. *et al.* Conditional vascular cell adhesion molecule 1 deletion in mice. Impaired lymphocyte migration to bone marrow. *J. Exp. Med.* **193**, 741–754 (2001).
47. Boggs, D.R. The total marrow mass of the mouse: a simplified method of measurement. *Am. J. Hematol.* **16**, 277–286 (1984).
48. Boak, J.L. & Woodruff, M.F.A. Modified technique for collecting mouse thoracic duct lymph. *Nature* **205**, 396–397 (1965).
49. Lyons, A.B. Analysing cell division in vivo and in vitro using flow cytometric measurement of CFSE dye dilution. *J. Immunol. Methods* **243**, 147–154 (2000).
50. Mempel, T.R., Scimone, M.L., Mora, J.R. & von Andrian, U.H. In vivo imaging of leukocyte trafficking in blood vessels and tissues. *Curr. Opin. Immunol.* **16**, 406–417 (2004).